

Addition formulas and the Rayleigh identity for arrays of elliptical cylinders

J. G. Yardley, R. C. McPhedran, N. A. Nicorovici

Department of Theoretical Physics, School of Physics, University of Sydney, New South Wales 2006, Australia

L. C. Botten

School of Mathematical Sciences, University of Technology Sydney, P. O. Box 123, New South Wales 2007, Australia

(Received 9 October 1998; revised manuscript received 25 May 1999)

We apply the Rayleigh method to solve the problem where a uniform electrostatic field is imposed upon a rectangular array of elliptical cylinders embedded in a matrix of unit dielectric constant. This new formulation overcomes geometric restrictions inherent in previous methods and is shown in principle and in various examples to converge for all possible geometries of the array and inclusion. Also presented are forms of both the interior and exterior addition formulas for harmonic functions in elliptical coordinates that possess optimal regions of convergence. [S1063-651X(99)03609-0]

PACS number(s): 03.50.De, 41.20.Cv, 78.20.Bh, 78.20.Ci

I. INTRODUCTION

This paper forms part of a systematic investigation of the generalization of a method due to Lord Rayleigh [1] for solving transport problems [2] of inhomogeneous media. The aim of the generalization is to extend Rayleigh's multipole technique to include geometries other than circles or spheres. This generalization is not straightforward, as is shown by the fact that our first attempt [3] at it in the context of a rectangular array of elliptical inclusions encountered an unexpected problem of convergence, resulting in an undesirable geometric restriction on the range of elliptical geometries that could be solved. It is the principal purpose of the present work to show how the geometric restriction can be lifted, and to demonstrate a generalization satisfactory in the sense of being capable of providing a solution to transport problems in all cases where ellipses do not intersect.

The precursor to this present work [3] was limited by the restriction illustrated in Fig. 1: that the branch cut associated with elliptical coordinates be circumscribed by a circle lying completely within the central unit cell. This problem occurred because a nonoptimal addition formula was used for the purpose of re-expressing the field arising from a general

inclusion (say, that centered on S in Fig. 2) in terms of fields associated with the central inclusion. [The term "addition theorem" is strictly intended to describe an algebraic equation which relates the values of a single function evaluated at the general arguments $u, v, u + v$. The coefficients in this algebraic equation must be independent of u, v . An "addition formula" is a (possibly transcendental) equation connecting three (possibly distinct) functions of the three arguments $u, v, u + v$. See [4].] The addition formula was nonoptimal because it involved a mixture of polar and elliptical coordinates and so exhibited a region of convergence inappropriate to a problem involving elliptical inclusions. Even when it is decided to use only harmonic functions of elliptical coordinates in addition formulas, our work has revealed that a specific procedure must be used to construct the addition formula which is optimal in the sense of applying in all problems involving nonintersecting ellipses. This optimal addition formula is derived precisely by using the Fourier expansion of the multipoles centered on S , in terms of the elliptical angular variable appropriate to the central ellipse.

The optimal addition formula is used to derive a Rayleigh identity: a system of linear equations whose solution determines the effective transport coefficient of the rectangular array, as well as the full form of the electrostatic field. We verify this formulation in a number of ways. First, we comment on the comparison between its results, those of our first

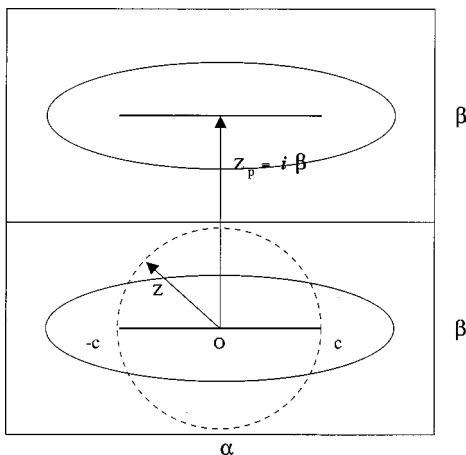


FIG. 1. Geometrical restriction inherent in our previous formulation.

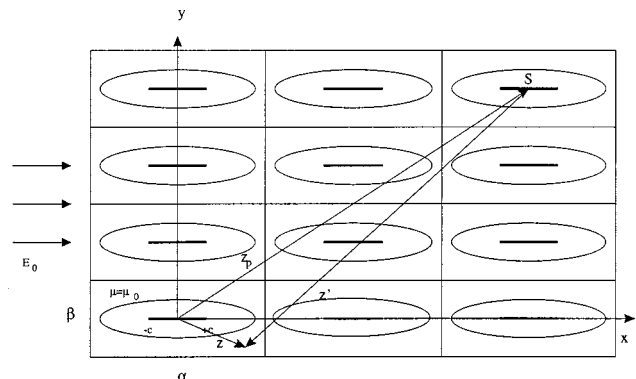


FIG. 2. Array of elliptical cylinders.

attempt [3], and numerical results obtained by Lu [5] using a boundary collocation method to determine the dielectric constant of highly elongated arrays with any filling fraction. Second, we verify Keller's reciprocal relationship [6,7] for this problem, and demonstrate numerically that in fact it is satisfied exactly, even when truncated field representations are used in the Rayleigh method. Third, we show that as the eccentricity $c \rightarrow 0$ and the elliptical coordinates become polar, the Rayleigh identity reduces to that which is appropriate for the problem involving circular inclusions [1]. We also exhibit the versatility of our formulation by showing results for the complex dielectric constant of various arrays of aluminum cylinders.

II. FIELD EXPANSIONS

The natural coordinates for transport problems involving elliptical cylinders where boundary matching must at some stage be performed are elliptical coordinates: ($\mu > 0, -\pi < \theta \leq \pi$). These are implicitly defined in terms of Cartesian coordinates by

$$z = x + iy = c \cosh w = c \cosh(\mu + i\theta). \quad (1)$$

This choice of coordinates allows the central elliptical inclusion to be defined by a single coordinate: $\mu = \mu_0$ (see Fig. 2) while the four fundamental basis functions for the complex potential are $e^{(\pm n\mu \pm in\theta)}$. However, simply representing the electrostatic potential as a series in these four functions introduces some redundancy and ignores a highly meaningful separation of field types based on the location of their respective sources. In short, all electrostatic fields can be decomposed into a part with its effective sources at infinity and a part with its effective sources on the local coordinate singularity.

Now, within the context of elliptical coordinates, that part of the field which has its sources at infinity must be regular over the central branch cut $\mu = 0$ while becoming singular at infinity. (A function is regular within a region if all of its derivatives and the function value itself are bounded. Within the context of two-dimensional complex potential functions, it should be noted that if a function is analytic in a region, then it is also regular there. Furthermore, unless otherwise specified, a "regular function" is one which has its only sources at infinity and an "irregular function" has its sources in the finite part of the plane.) A simple calculation shows that only linear combinations of the four fundamental basis solutions, $e^{(\pm n\mu \pm in\theta)}$, that can be expressed as linear combinations of $\cosh nw$ are regular on the branch cut. All other linear combinations of the fundamental solutions have singularities in the first derivative (electric field) at the branch points. As a result, the regular basis function is uniquely determined to be $\cosh nw$ and so the expansion of the field in the region interior to the inclusion is

$$\mathcal{V}_i = \sum_{n=0}^{\infty} \epsilon_n \left(\frac{c}{2}\right)^n C_n \cosh nw, \quad (2)$$

where ϵ_n is the Neumann symbol ($\epsilon_0 = 1, \epsilon_n = 2\forall n > 0$).

Similarly, that part of the field which is regular at infinity and so has its sources along the branch cut must be a linear

combination of the function e^{-nw} , since all other analytic combinations of the four fundamental solutions involve e^{nw} and so become singular at infinity. Therefore, the irregular basis function, e^{-nw} , is also uniquely determined so that the field expansion in the region of the central unit cell exterior to the inclusion is

$$\mathcal{V}_e(c \cosh w) = A_0 + \sum_{n=1}^{\infty} \left[\epsilon_n \left(\frac{c}{2}\right)^n A_n \cosh nw + \left(\frac{2}{c}\right)^n B_n \exp -nw \right]. \quad (3)$$

It is useful for calculations to represent the potentials as functions of z which, under the coordinate transformation $z = c \cosh w$, reduce identically to the above representation. That is,

$$\mathcal{V}_i(z) = \sum_{n=0}^{\infty} \epsilon_n \left(\frac{c}{2}\right)^n C_n T_n\left(\frac{z}{c}\right), \quad (4)$$

$$\mathcal{V}_e(z) = A_0 + \sum_{n=1}^{\infty} \left[\epsilon_n \left(\frac{c}{2}\right)^n A_n T_n\left(\frac{z}{c}\right) + \left(\frac{2}{c}\right)^n B_n V_n\left(\frac{z}{c}\right) \right], \quad (5)$$

where $T_n(z)$ is the n th Chebyshev polynomial and

$$V_n\left(\frac{z}{c}\right) = \exp\left(-n \cosh^{-1} \frac{z}{c}\right) \quad (6)$$

$$= \left(\frac{z}{c} + \sqrt{\frac{z}{c} - 1} \sqrt{\frac{z}{c} + 1}\right)^{-n} \\ = \left(\frac{z}{c} - \sqrt{\frac{z}{c} - 1} \sqrt{\frac{z}{c} + 1}\right)^n \quad (7)$$

$$= 2^{-n} \left(\frac{z}{c}\right)^{-n} {}_2F_1\left[\frac{n+1}{2}, \frac{n}{2}; n + 1; \left(\frac{c}{z}\right)^2\right]. \quad (8)$$

Both series representations (3),(5) for \mathcal{V}_e can be shown to converge absolutely in an elliptical annulus properly including the boundary of the physical inclusion $\mu = \mu_0$ while the two representations (2),(4) for \mathcal{V}_i converge absolutely inside an elliptical region properly containing $\mu = \mu_0$. Also, both the functions T_n, V_n satisfy appropriate orthogonality relations on a given fixed ellipse, although it is a trivial matter to apply Cauchy's theorem and represent the inner products of T_n, V_n as contour integrals around any contour that contains the branch cut $(-c, +c)$:

$$\oint \frac{T_n\left(\frac{z}{c}\right) T_m\left(\frac{z}{c}\right)}{\sqrt{z+c} \sqrt{z-c}} dz = \frac{2\pi i \delta_{n,m}}{\epsilon_n}, \quad (9)$$

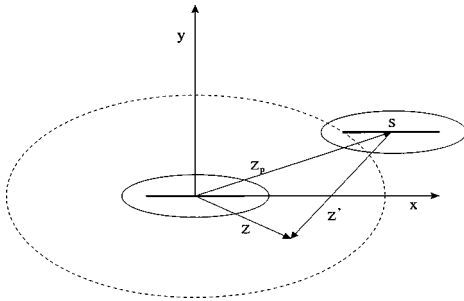


FIG. 3. Geometry of the interior addition formula.

$$\oint \frac{V_n\left(\frac{z}{c}\right) T_m\left(\frac{z}{c}\right)}{\sqrt{z+c}\sqrt{z-c}} dz = \frac{2\pi i \delta_{n,m}}{\epsilon_n}, \quad (10)$$

$$\oint \frac{V_n\left(\frac{z}{c}\right) V_m\left(\frac{z}{c}\right)}{\sqrt{z+c}\sqrt{z-c}} dz = 2\pi i \delta_{n,m}. \quad (11)$$

Note that it is essential for the correct treatment of the branch cut that the weight function be represented exactly as shown in Eqs. (9),(10) and not as $\sqrt{z^2-c^2}$.

III. THE ADDITION FORMULA

It is of fundamental importance to the Rayleigh method that there exists a convergent interior addition formula which can be applied to any problem involving nonintersecting ellipses. Such a formula would allow the field due to cylinders such as that centered on S (Figs. 2 and 3) to be expanded in terms of regular functions about the origin provided that the field point z lay inside the biggest ellipse which completely excludes the branch cut associated with S (see Fig. 3). [Note that the actual ellipses shown in Fig. 3 (solid lines) are nothing more than a decoration—it is the position of the branch cut at S and the field point that determine the convergence properties of the interior addition formula. The solid ellipses may intersect without necessarily effecting the convergence of the addition formula.] Symbolically, the expansion is of the form

$$V_n\left(\frac{z}{c} - \frac{z_p}{c}\right) = \sum_{s=0}^{\infty} \beta_s^n\left(\frac{z_p}{c}\right) T_s\left(\frac{z}{c}\right). \quad (12)$$

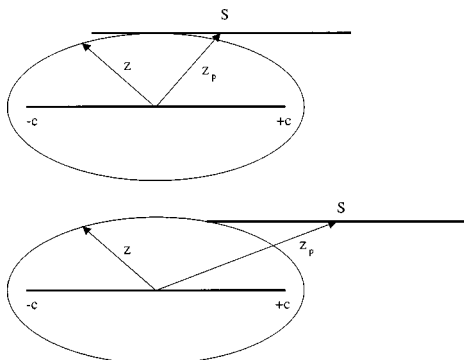


FIG. 4. Critical geometries for the addition formula.

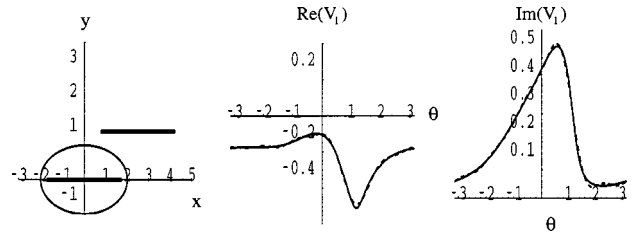


FIG. 5. A continuous projection with, in the center and middle figures, the solid line denoting the function V_1 and the dashed line its Fourier series.

To see that the expansion (12) is capable of representing an optimally convergent interior addition formula, observe that, for a given z_p , the right-hand side of Eq. (12) has the form of a Fourier expansion on the surface of the central ellipse. As such, the coefficients are defined by the standard projection integral and so all that is needed for this series to converge uniformly and absolutely is that the function be represented, $V_n[(z/c) - (z_p/c)]$, be smooth on the boundary of the central ellipse. This will be true in general if the inclusions are nonintersecting because the source points for the field generated by each inclusion cannot lie outside that inclusion. In fact, for the case of elliptical inclusions, these source points lie on the branch cut at the center of each source ellipse, so that the smoothness of $V_n[(z/c) - (z_p/c)]$ on the central ellipse is guaranteed provided $z - z_p \notin (-c, c)$ or, equivalently, that $\text{Re}\{\cosh^{-1}[(z - z_p)/c]\} \neq 0$ (see Fig. 4). This is clearly the case provided that the ellipses do not intersect, as can be seen in the following sequence of plots (Figs. 5 and 6) in which the field $V_1[(z/c) - (z_p/c)]$ is considered to be emanating from sources on the branch cut at z_p .

From left to right we have the geometry of the situation; the real part of both the exact projection (full line) and the series (2) reconstruction (dashed line) of this projection; the imaginary part of the exact projection displaying the projection of the field onto the central ellipse and the corresponding series representation (2). For the first geometry the exact projection and its reconstruction can be seen to be almost identical after including only five terms in the series (2). However, in the second geometry the previously described restrictions are violated as the branch cut centered on z_p enters the central ellipse and the series is seen not to converge to the correct result.

The representation and calculation of the $\beta_s^n(z_p)$ is an intricate matter requiring care. Indeed, in view of the previous work involving circular or spherical inclusions [1], the most obvious generalization of the Rayleigh method would suggest the use of an addition formula of the form

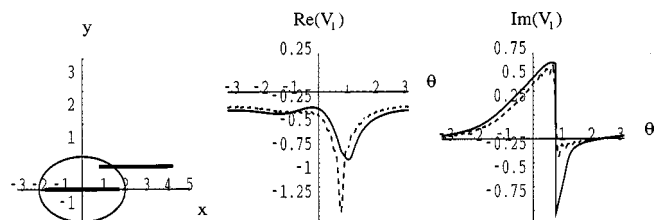


FIG. 6. A discontinuous projection with, in the center and middle figures, the solid line denoting the function V_1 and the dashed line its Fourier series.

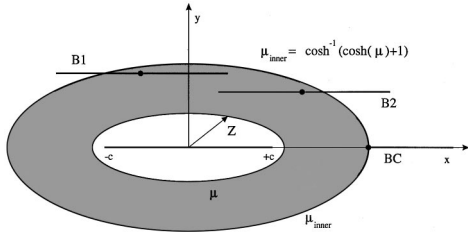


FIG. 7. Convergence of the addition formula written as a double series.

$$V_n\left(\frac{z}{c} - \frac{z_p}{c}\right) = \sum_{s=1}^{\infty} \sum_{r=1}^{\infty} c_{r,s}^n V_r\left(\frac{z_p}{c}\right) T_s\left(\frac{z}{c}\right). \quad (13)$$

Such a representation would of course result in a series for the $\beta_s^n(z_p/c)$ in terms of the irregular basis functions, $V_k(z_p)$, and in turn would lead to the seemingly natural identification of the lattice sums as a sum over the lattice of this irregular basis function. However, as will be shown, this form (13) of the addition formula and the corresponding expansion of the $\beta_s^n(z_p/c)$ in series of irregular functions do not converge absolutely in an optimal region. The following argument proves this by contradiction.

Suppose one requires absolute convergence of the double series (13). It is then clear that the convergence or otherwise can only depend on the two radial coordinates μ, μ_p . Indeed, the ratio test shows that absolute convergence can be expected for μ less than some value, μ_{outer} , and μ_p greater than some value μ_{inner} . However, as indicated in Fig. 4, the best that can be hoped for from any addition formula corresponds to the situation where convergence is observed as long as the branch cut centered on z_p does not touch the coordinate ellipse passing through z . This would require μ_{inner} to depend on the elliptical phase of z_p and so we conclude that Eq. (13) cannot converge absolutely in this optimum region.

In fact, the maximum region of convergence of Eq. (13) can be determined by considering a fixed value of μ th coordinate ellipse passing through the field point z and allowing the value of μ_p to decrease while the field point z_p slides around its coordinate line. It is clear from the critical situation shown in Fig. 7 that the first time a singularity is encountered will be when θ_p is zero and the source branch cut (BC) is just touching the ellipse along its major axis. This situation defines μ_{inner} and in fact $\cosh\mu_{inner} = \cosh\mu + 1$. As a result, the series (13) will not converge absolutely (in fact it diverges) for arrangements where the center of the source ellipse, z_p , is within the shaded region of Fig. 7 (B1),(B2) even though the ellipses may not intersect. Note also that this restriction means that μ_p must always be greater than $\cosh^{-1}(\cosh\mu + 1) > \cosh^{-1}2$ in order for the representation (13) to be valid. In particular, this implies that the vertical spacing of a regular array defined by the vectors z_p must be greater than $\sqrt{3}c$ in order for this form of the addition formula to be applicable. This restriction is an improvement over that obtained by Nicorovici and McPhedran [3], which requires this vertical spacing to be greater than $2c$, although it is still far from optimal, since solutions to a large subset of array problems involving nonintersecting ellipses cannot be solved while this restriction remains.

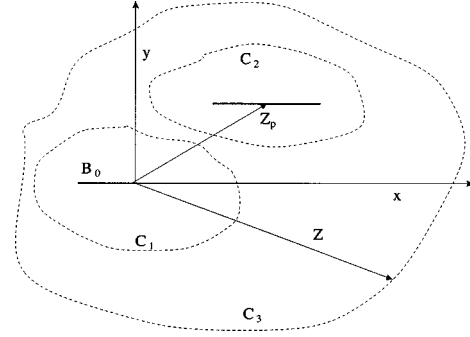


FIG. 8. Paths of integration used to determine various Fourier coefficients.

The outer radius of convergence, μ_{outer} , is determined in a similar fashion by fixing a particular value of the source point and allowing the field point z to slide around its coordinate ellipse μ as this ellipse is enlarged. In what is an almost identical situation to that described above, the first singularity is encountered on the x axis when $\cosh\mu_{outer} = \cosh\mu_p - 1$. This restriction is really just a restating of that involving μ_{inner} , the only difference being that now the field point is considered to be the ‘‘active’’ variable in Eq. (13).

The correct approach for calculating the coefficients $\beta_s^n(z_p/c)$ in this case, and in fact the optimal route to a convergent representation for inclusions of any shape, is obtained through the use of the orthogonality relation (10) on the curve C_1 (see Fig. 8). Provided that the branch cut centered on z_p remains entirely outside the path of integration, this yields the convergent integral representation

$$\beta_s^n\left(\frac{z_p}{c}\right) = \frac{\epsilon_s}{2\pi i} \oint \frac{V_n\left(\frac{z-z_p}{c}\right) T_s\left(\frac{z}{c}\right)}{\sqrt{z+c}\sqrt{z-c}} dz. \quad (14)$$

This integral can be collapsed onto the branch cut B_0 of Fig. 8 and transformed using elliptical coordinates to give an alternate form which is superior for numerical purposes:

$$\beta_s^n\left(\frac{z_p}{c}\right) = \frac{\epsilon_s}{2\pi} \int_{-\pi}^{\pi} V_n\left(\cos\theta - \frac{z_p}{c}\right) \cos(s\theta) d\theta. \quad (15)$$

Although such an integral form can be used safely in a Rayleigh formulation, a series expansion that is valid in the optimum region and therefore equivalent to Eq. (14) is in some ways preferable. Even though its derivation is not on quite as solid a footing as the above integral representation, it is possible to derive a series representation which is found to be absolutely convergent in an optimal region. Such a series can be derived in terms of Gaussian hypergeometric functions by either differentiating the expansion of the field due to a monopole or by manipulating certain series involving hypergeometric functions (see Appendix A). One form of the result is

$$\begin{aligned} \beta_s^n\left(\frac{z_p}{c}\right) &= (-1)^n \epsilon_s \sum_{m=0}^{\infty} \frac{(2m+s+n-1)!}{m!(m+s)!(n-1)!} \\ &\times V_{n+2m+s}\left(\frac{z_p}{c}\right) {}_2F_1 \\ &\times \left[2m+s+n, 2m+s; n+1; V_2\left(\frac{z_p}{c}\right) \right]. \end{aligned} \quad (16)$$

This series converges absolutely for all values of $\mu_p > 0$. However, if the hypergeometric function is expanded using the standard power series expansion [8], then even though $|V_2(z_p)| = e^{-\mu_p} < 1$ and the power series itself converges absolutely for all μ_p , the double series obtained for $\beta_s^n(z_p/c)$ will only be conditionally convergent if $0 < \mu_p < \cosh^{-1}2$. Furthermore, attempts made at manipulating the form of the series (16) by using the linear and quadratic transformations that apply to hypergeometric functions of the form ${}_2F_1(a, b, a-b+1; z)$, and various expansions of these hypergeometric functions, did not alter this property of conditional convergence. [Some of these manipulations, and in particular one in which the hypergeometric function in Eq. (16) is transformed into a terminating hypergeometric function, are shown in the Appendices.] As such, it is likely that if the series (16) is to be considered as a double series in elementary functions, then the arrangement of terms implicit in the form (16) is the unique one which produces a double series that is convergent for all values of $\mu_p > 0$.

IV. FIELD AND RAYLEIGH IDENTITIES

A. Field identity and lattice sums

The field identity is the essence of the Rayleigh method in that it provides a relationship connecting the regular part of the field about a particular inclusion with the irregular field that has its sources located at all the other cylinder centers [1]. In this particular problem, and with reference to the field expansion (5), the field identity has the form

$$\sum_{n=1}^{\infty} \epsilon_n \left(\frac{c}{2}\right)^n A_n T_n\left(\frac{z}{c}\right) = -\bar{E}_0 z + \sum_{p \neq 0} \sum_{n=1}^{\infty} \left(\frac{2}{c}\right)^n B_n V_n\left(\frac{z'}{c}\right), \quad (17)$$

where $E_0 = E_x + iE_y$ is the incident electric field and $z' = z - z_p$, while the sum over the index p includes all but the central cylinder.

One way of deriving Eq. (17) is to use Liouville's theorem, which states that the difference between an analytic function and the sum of its singular parts (either in the finite part of the plane or at infinity) must be a constant. Now, due to the translational symmetry in the array, the coefficients A_n, B_n, C_n in Eq. (5) are the same when the field is expanded about any cylinder in the lattice (an exception to this is $A_0 = -\bar{E}_0 z_p$, which is cylinder dependent because of the external field). Consequently, the contributions from all cylinders in the lattice can be combined to give

$$\sum_p \sum_{n=1}^{\infty} \left(\frac{2}{c}\right)^n B_n V_n\left(\frac{z'}{c}\right), \quad (18)$$

where $z' = z - z_p$ and this time z_p ranges over every cylinder in the array. The only singularity at infinity is due to the incident field and so we have

$$\mathcal{V}_e(z) - \sum_p \sum_{n=1}^{\infty} \left(\frac{2}{c}\right)^n B_n V_n\left(\frac{z'}{c}\right) - (-\bar{E}_0 z) = 0. \quad (19)$$

This reduces to Eq. (17) after substituting Eq. (5) and making the choice $A_0 = 0$.

We now wish to reduce the field identity (17) to a set of linear equations connecting the coefficients A_n and B_n of Eq. (5). We do this by imposing Eq. (17) on a contour traced out by the field point z where the addition formula is everywhere valid. Such a contour is provided by an ellipse with $\mu = \delta + \mu_0$ for $\delta > 0$ a small positive number. In all but the case where the inclusions actually touch, this contour can be chosen to properly contain the physical inclusion and itself be properly contained by the unit cell. It is straightforward to verify that, provided δ is chosen to be small enough, the order condition on the addition formula (see Fig. 4),

$$\mu_0 < \min_{-\pi < \alpha \leq \pi} \operatorname{Re} \left[\cosh^{-1} \left(\frac{z_p}{c} - \cos \alpha \right) \right], \quad (20)$$

is satisfied for every array of nonintersecting ellipses.

Applying the addition formula (12) and equating coefficients of $T_s(z/c)$ in Eq. (17) yields the final form of the field identity:

$$A_s = -\bar{E}_0 \delta_{s,1} + \sum_{n=1}^{\infty} \sigma(n,s) B_n, \quad (21)$$

where we have introduced elliptic lattice sums defined by

$$\sigma(n,s) = \frac{1}{\epsilon_s} \left(\frac{2}{c}\right)^{n+s} \sum_{p \neq 0} \beta_s^n\left(\frac{z_p}{c}\right). \quad (22)$$

These sums are the direct analogue of the lattice sums introduced for the circular problem [1]. As for their circular counterparts, in an array with rectangular symmetry where z_p and \bar{z}_p are both lattice vectors, we have that all the sums must be real. Furthermore, all arrays possess symmetry under the operation $z_p \rightarrow -z_p$ so that only even values of the sum $n+s$ yield a nonzero value for $\sigma(n,s)$. All the lattice sums are absolutely convergent except for $\sigma(1,1)$, which is the elliptical equivalent of the conditionally convergent S_2 [1]. The numerical problems arising from this conditional convergence can be overcome through the use of Kummer's method for converting a conditionally convergent series into an absolutely convergent one by subtracting a known sum. Specifically, by using the fact that for small c we have (see Appendix B)

$$\sigma(n,s) \sim (-1)^n \binom{s+n-1}{s} S_{n+s}, \quad (23)$$

and that S_2 can be evaluated using the absolutely convergent series given in [1], we can represent $\sigma(1,1)$ as an absolutely convergent series:

$$\sigma(1,1) = -S_2 + \sum_{p \neq 0} \left[\frac{1}{2} \left(\frac{2}{c} \right)^2 \beta_1^1 \left(\frac{z_p}{c} \right) + z_p^{-2} \right]. \quad (24)$$

It should be noted that the value of this conditionally convergent lattice sum changes depending on whether one is solving for the x component of the applied field or the y component. This is because the physically correct interpretation of the conditionally convergent sum $\sigma(1,1)$ requires the summation over needle-shaped regions oriented along the line of the applied field [1].

B. Boundary conditions and the Rayleigh identity

A second set of relations between the coefficients A_n, B_n may be obtained through the application of boundary conditions on the surface of the central inclusion, μ_0 . These are

$$\text{Re}(\mathcal{V}_e)|_{\mu=\mu_0} = \text{Re}(\mathcal{V}_i)|_{\mu=\mu_0}, \quad (25)$$

$$\left. \frac{\partial \text{Re}(\mathcal{V}_e)}{\partial \mu} \right|_{\mu=\mu_0} = \epsilon \left. \frac{\partial \text{Re}(\mathcal{V}_i)}{\partial \mu} \right|_{\mu=\mu_0}, \quad (26)$$

where ϵ is the relative dielectric constant of the elliptic inclusions. Now, the complex coefficients A_s, B_s naturally decompose into their real and imaginary parts which correspond to the parts of the solution which are, respectively, symmetric (e) and antisymmetric (o) about the x axis. So, on writing: $A_s = A_s^e - iA_s^o$, $B_s = B_s^e + iB_s^o$, and $C_s = C_s^e - iC_s^o$, Eqs. (25),(26) become (for $s > 0$)

$$A_s^e = \frac{\cosh s\mu_0 + \epsilon \sinh s\mu_0}{(1-\epsilon)\sinh 2s\mu_0} \left(\frac{2}{c} \right)^{2s} e^{-s\mu_0} B_s^e, \quad (27)$$

$$C_s^e = \frac{1}{(1-\epsilon)\sinh 2s\mu_0} \left(\frac{2}{c} \right)^{2s} B_s^e, \quad (28)$$

$$A_s^o = \frac{\epsilon \cosh s\mu_0 + \sinh s\mu_0}{(1-\epsilon)\sinh 2s\mu_0} \left(\frac{2}{c} \right)^{2s} e^{-s\mu_0} B_s^o, \quad (29)$$

$$C_s^o = \frac{1}{(1-\epsilon)\sinh 2s\mu_0} \left(\frac{2}{c} \right)^{2s} B_s^o. \quad (30)$$

When combined with the field identity (21), we have two Rayleigh identities—one resulting from the field component along the x axis and one from that along the y axis [9,3]:

$$\begin{aligned} & \frac{\cosh s\mu_0 + \epsilon \sinh s\mu_0}{(1-\epsilon)\sinh 2s\mu_0} \left(\frac{2}{c} \right)^{2s} e^{-s\mu_0} B_s^e \\ &= -E_0^x \delta_{s,1} + \sum_{n=1}^{\infty} \sigma(n,s) B_n^e, \end{aligned} \quad (31)$$

$$\begin{aligned} & \frac{\epsilon \cosh s\mu_0 + \sinh s\mu_0}{(1-\epsilon)\sinh 2s\mu_0} \left(\frac{2}{c} \right)^{2s} e^{-s\mu_0} B_s^o \\ &= -E_0^y \delta_{s,1} - \sum_{n=1}^{\infty} \sigma(n,s) B_n^o. \end{aligned} \quad (32)$$

After tabulating the elliptical lattice sums, $\sigma(n,s)$, and taking particular care to calculate the value of $\sigma(1,1)$ that is

appropriate for each of the two linear systems (31), (32), both systems can be solved to yield the coefficients B_n^e and B_n^o . An application of Green's theorem on the boundary of the region between the inclusion and the unit cell boundary gives the components of the homogenized dielectric tensor [3]:

$$\epsilon_x^* = 1 + 2\pi \frac{B_1^e}{E_0^x \alpha \beta}, \quad (33)$$

$$\epsilon_y^* = 1 + 2\pi \frac{B_1^o}{E_0^y \alpha \beta}. \quad (34)$$

V. NUMERICAL RESULTS

In both of the following applications of our formulation, we follow the same basic numerical procedure, the only difference being that in the first we utilize only the integral representation (15) for the β_s^n and in the second a hybrid representation involving both the integral representation and the series representation (16) is used. All numerical calculations were carried out using MATHEMATICA 3.0. The first step is to calculate the lattice sums for a particular lattice geometry (and value of c) using Eq. (24). There are two approximations involved here: first, the β_s^n are not known exactly but one of either the series or integral representation must be used to approximate these coefficients, and second, the actual summation over the lattice must be truncated at some stage. These approximate lattice sums [$\sigma(n,s)$] are used in the pair of infinite linear systems (31), (32) (Rayleigh identities), which are also truncated before a simple matrix inversion yields the coefficients $B_n^{(e,o)}$ and in particular $B_1^{(e,o)}$. These allow the calculation of the effective dielectric tensor through (33),(34).

A. Arrays of aluminum cylinders

Using the above procedure and the integral representation (15) of the β_s^n , we calculate the dielectric constant for certain arrays of aluminum cylinders. (All integrals were calculated using the numerical integration packages that are standard in MATHEMATICA 3.0.) The experimentally determined dispersion relation for aluminum [10] can be used to produce plots of the real and imaginary parts of the effective dielectric constant for the array as a function of wavelength. The following plots show the real and imaginary parts of the dielectric constant for aluminum as a function of wavelength (microns).

Now, for each point on the above dispersion curve (Fig. 9) we calculate a variety of results subject to the numerical restrictions arising from the truncation of the Rayleigh identity (31),(32) to fifth order; the truncation of the lattice sum series to 10th order (i.e., a square of side length 10); and the calculation of the β_s^n to an accuracy of 1 part in 10^5 . The stability of this numerical approximation is strongly dependent on the filling fraction of the cylinders within the unit cell, but is typically accurate to the third or fourth significant figure. This precision can be improved but the procedure quickly becomes very time consuming.

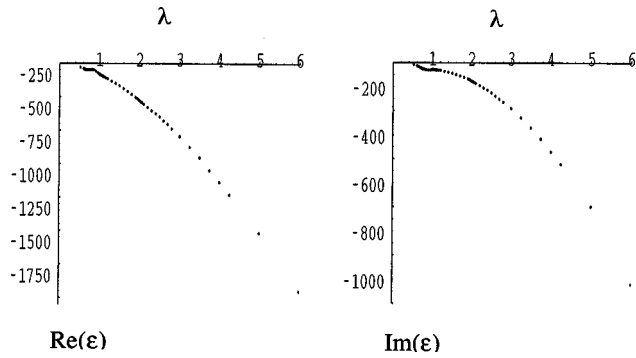


FIG. 9. Aluminium dispersion curve. The wavelength (λ) is in microns.

The first pair of plots (Fig. 10) show the real and imaginary parts of the x component of the effective dielectric constant [$\epsilon_x^*(\epsilon)$]. The second pair shows the real and imaginary parts of the y component of the effective dielectric constant [$\epsilon_y^*(1/\epsilon)$] for an array where the individual cylinders are now considered to have a dielectric constant of $1/\epsilon$.

These results (Fig. 10) satisfy Keller's Reciprocal Law [6,7] to within 1%. Briefly, Keller's law states that if the components of the dielectric tensor are considered to be functions of the dielectric constant of the inclusions, ϵ , then

$$\epsilon_x^*(\epsilon) \epsilon_y^*\left(\frac{1}{\epsilon}\right) = 1. \quad (35)$$

As previous Rayleigh formulations for circular inclusions have confirmed analytically [11], Keller's law is found to be satisfied (subject to the accuracy of calculation in determining the β_s^n) even for finite truncation orders of the Rayleigh identity (31),(32). This has the consequence that within the context of a Rayleigh formulation, Keller's law can only be regarded as a test of self-consistency and as such stability in the final numerical result for the effective dielectric constant must be obtained independently of, and in addition to, agreement with Keller's law. This effect is observed here numeri-

cally inasmuch as the deviations from Eq. (35) are independent of the order of truncation of the Rayleigh identity (31),(32).

Shown below are further tests of the formulation for successively more demanding situations (Figs. 11–13). The various truncation orders used to obtain Fig. 10 have been left unchanged. It is found that in all of these cases, Keller's law is satisfied to within 1% over the entire range of wavelengths and that the dielectric constant itself is accurate to at least three significant figures.

B. Verification of Lu's results

We also present here some results for highly rectangular arrays where the aspect ratio of both the inclusion and ellipse is 10 to 1 and the dielectric constant is real. This case was studied by Lu [5] and almost all of his results are confirmed using the numerical procedure described above with the numerically efficient hybrid representation of the β_s^n .

The unbracketed numbers in Table I were obtained using this hybrid representation of the β_s^n in which nearby inclusions are included in the lattice sums using the integral representation, while the more distant ones are included using the series representation. These results agree with those of Lu [5] for all filling fractions shown and were obtained by requiring at least six significant figures of accuracy in both the calculation of the β_s^n and the resulting lattice sums (24), while the Rayleigh identity was truncated to ninth order.

In addition to reproducing Lu's results using the hybrid representation, we demonstrate the typical performance of the formulation using only the series representation (16) truncated after 20 terms. These are the bracketed numbers of Table I and were produced by requiring stability in the lattice sums to about 1 part in 10^4 and using a fifth-order truncation of the Rayleigh identity. Note that if only the series representation is used, the increases in numerical precision required to reach an accuracy of four significant figures using the series (16) in the cases where the filling fraction is greater than 0.72 makes these calculations very time consuming.

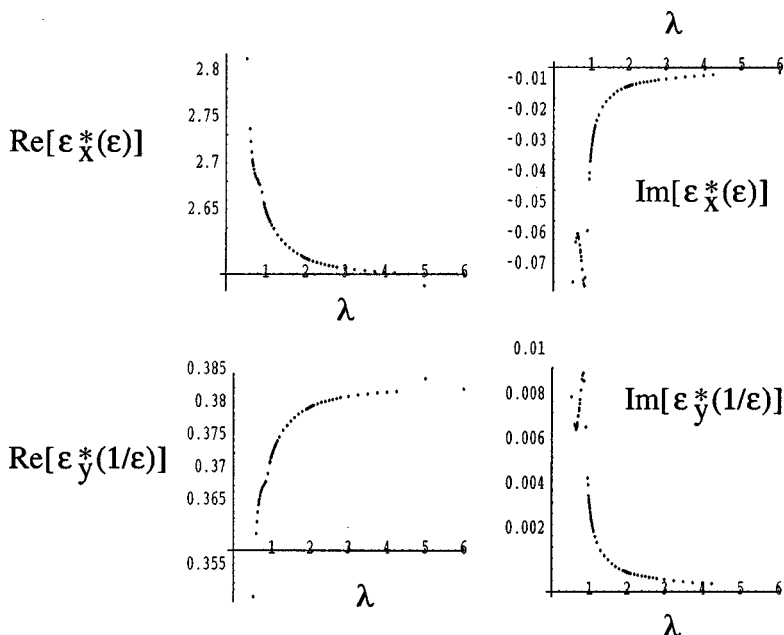


FIG. 10. Effective response as a function of the wavelength, λ (microns) for an array with parameters $\alpha=2$, $\beta=1$, and a filling fraction of 0.4.

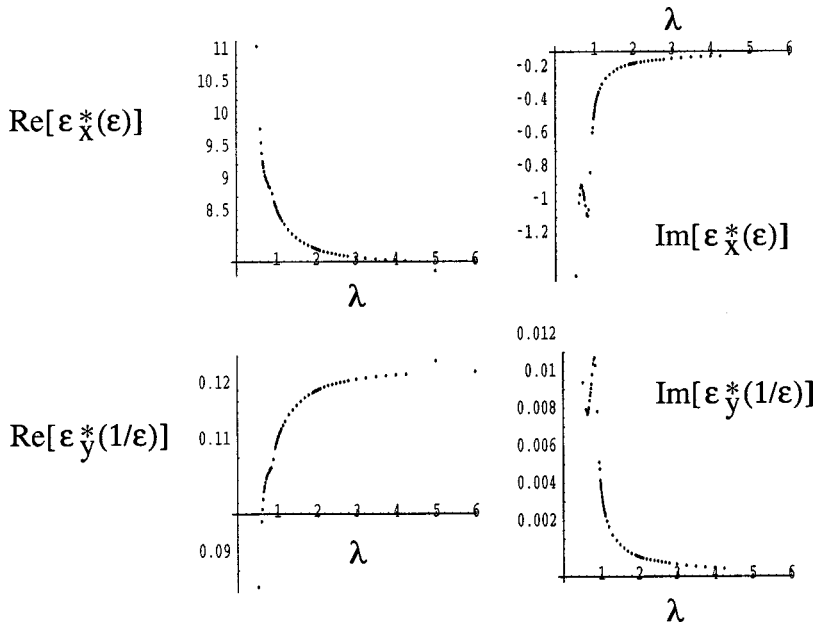


FIG. 11. Effective response as a function of the wavelength, λ (microns) for an array with parameters $\alpha=2, \beta=1$, and a filling fraction of 0.7

The reason that the series representation (16) produces inaccurate results for large filling fractions is that in cases such as this, with high array and inclusion aspect ratios, there is a large degree of cancellation in the calculation of the hypergeometric function [see Appendix C and, in particular, Eq. (C7)] for values of z_p that are purely imaginary and of magnitude less than $2c$. Therefore, in the region ($|z_p| < 2c$) the slower but more stable integral representation (15) is used.

Finally, we note that Keller's reciprocal law is satisfied to within 1% for all cases shown in Table I, i.e., $|\epsilon_x^*(5)\epsilon_y^*(0.2) - 1| < |\epsilon_x^*(50)\epsilon_y^*(0.02) - 1| < 0.01$. Once again, we observe that the agreement with Keller's law is independent of the truncation order of the Rayleigh identity (31),(32).

VI. CONCLUSIONS

We have exhibited a Rayleigh formulation for this transport problem involving rectangular arrays of ellipses which

is convergent for all geometries of the array and ellipse and in so doing we have extended and completed the previous work on this problem using the Rayleigh method [3]. As such, we have given the first completely successful example of the extension of Rayleigh's technique to noncircular/spherical geometries. Furthermore, in the course of obtaining this solution, a new addition formula for harmonic functions in elliptical coordinates was derived by taking the clear view of the addition formula as simply a Fourier expansion about the central inclusion. This improved understanding of the role of the addition formula makes clear the validity of the Rayleigh method in the general case where the inclusion is of arbitrary shape because any smooth function (i.e., with continuous first and second derivatives) possesses an absolutely and uniformly convergent Fourier series. Finally, our method is applicable to dynamic problems and should remove the restrictions currently preventing a full solution for problems involving the scattering of waves by two or more ellipses [12].

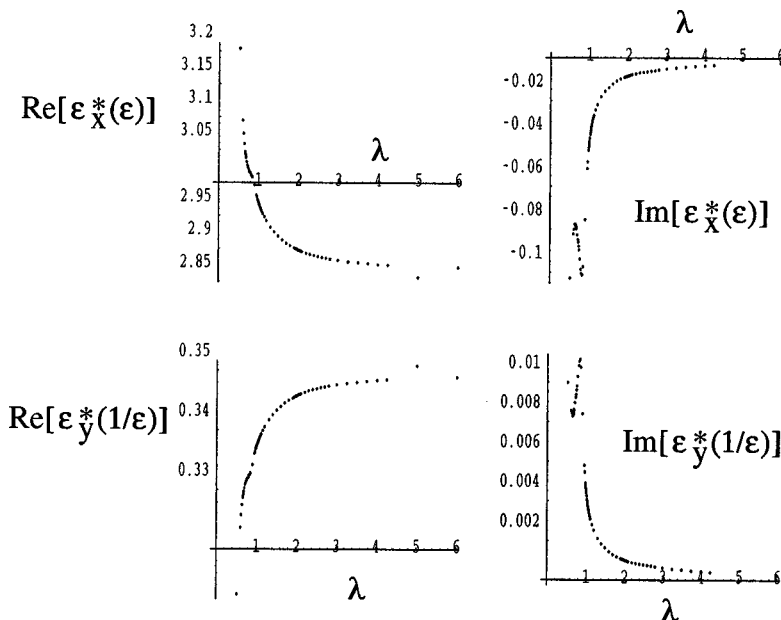


FIG. 12. Effective response as a function of the wavelength, λ (microns) for an array with parameters $\alpha=4, \beta=1$, and a filling fraction of 0.4.

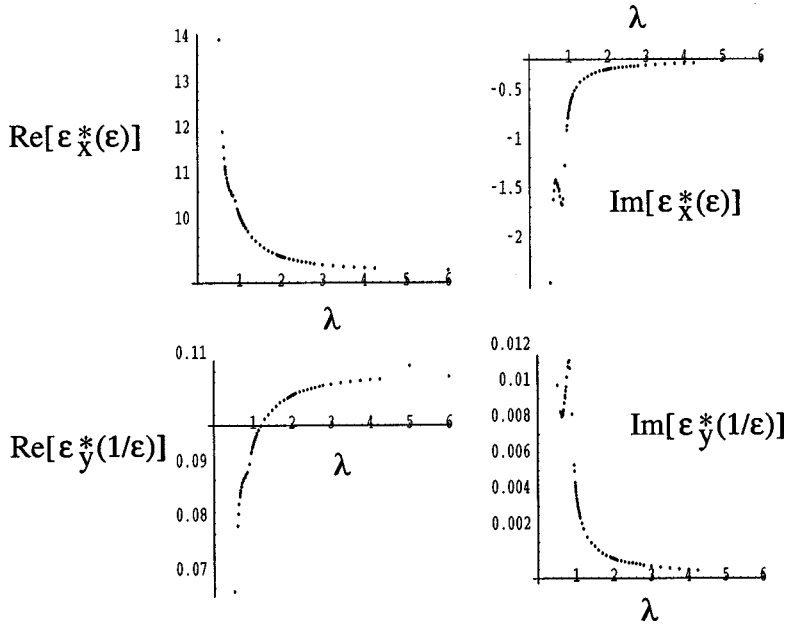


FIG. 13. Effective response as a function of the wavelength, λ (microns) for an array with parameters $\alpha=4$, $\beta=1$, and a filling fraction of 0.7.

ACKNOWLEDGMENTS

This work was supported by the Australian Postgraduate Award Scheme (J.Y.) and by the Australian Research Council (N.N. and R.C.McP.). Helpful discussions with Professors A. B. Movchan and G. W. Milton are also acknowledged. The authors also acknowledge the provision of a beta test version of MATHEMATICA 3.0 from Wolfram Research, Inc.

APPENDIX A: DERIVATION OF THE β_s^n

The method for deriving the integral representation (15) of the $\beta_s^n(z_p)$ using the orthogonality relation (10) is very straightforward, although this representation is not numerically efficient when the source point is further than about $2c$ from the origin. Therefore, it is important for this and other reasons to have an alternative representation as a series. We present here the two main methods used to derive series such

as (16) for the $\beta_s^n(z_p)$, although it should be realized that, because of the large number of linear and quadratic transformations linking various hypergeometric functions, there are many equivalent forms possible.

1. Analytic continuation of a Taylor series

For a fixed z_p the Taylor expansion

$$V_n(z-z_p) = \sum_0^{\infty} \frac{\partial^m}{\partial z^m} V_n(z-z_p) \Big|_{z=0} \frac{z^m}{m!} \quad (\text{A1})$$

will converge inside some circle in the z plane. So, on writing

$$V_n(z-z_p) = 2^{-n} (z-z_p)^{-n} {}_2F_1 \left[\frac{n+1}{2}, \frac{n}{2}; n+1; \left(\frac{1}{z-z_p} \right)^2 \right] \quad (\text{A2})$$

TABLE I. Lu's results for the effective response of array with dimensions $\alpha=10$, $\beta=1$, and various filling fractions f .

f	$\epsilon_x^*(5)$	$\epsilon_y^*(0.2)$	$\epsilon_x^*(50)$	$\epsilon_y^*(0.02)$
0.1	1.216	0.8223	1.433	0.6978
0.2	1.417	0.7056	1.817	0.5504
0.3	1.639	0.6100	2.288	0.4370 (0.4371)
0.4	1.899	0.5267	2.930 (2.929)	0.3413 (0.3414)
0.5	2.214	0.4517 (0.4516)	3.892 (3.894)	0.2569 (0.2568)
0.55	2.400 (2.401)	0.4167 (0.4165)	4.589 (4.593)	0.2179 (0.2177)
0.6	2.611 (2.612)	0.3829 (0.3828)	5.536 (5.544)	0.1806 (0.1804)
0.64	2.802 (2.803)	0.3568 (0.3567)	6.584 (6.593)	0.1519 (0.1517)
0.67	2.961 (2.962)	0.3377 (0.3376)	7.641 (7.650)	0.1309 (0.1307)
0.7	3.136 (3.137)	0.3189 (0.3188)	9.073 (9.078)	0.1102 (0.1102)
0.72	3.262 (3.263)	0.3065 (0.3064)	10.36 (10.36)	0.09648 (0.9654)
0.74	3.400 (3.401)	0.2941 (0.2941)	12.12 (12.08)	0.08250 (0.08277)
0.75	3.475 (3.474)	0.2878 (0.2878)	13.29 (13.21)	0.07522 (0.07571)
0.76	3.554 (3.552)	0.2814 (0.2815)	14.81 (14.62)	0.06750 (0.06841)
0.77	3.641 (3.636)	0.2746 (0.2751)	16.99 (16.47)	0.0588 (0.06073)

and utilizing formulas given in [13], we have that

$$\frac{\partial^m}{\partial z^m} V_n(z-z_p)|_{z=0} = (-1)^n 2^m n^{(m)} V_{n+m}(z_p) {}_2F_1 \\ \times (m+n, m; n+1; V_2(z_p)), \quad (\text{A3})$$

where $n^{(m)} = n(n+1)(n+2)\cdots(n+m-1)$ is the Pochhammer symbol.

Now, the standard polynomials z^m can be expanded in terms of Chebyshev polynomials as

$$z^m = \frac{1}{2^m} \sum_{p=0}^m e_{m-p} \epsilon_p \binom{m}{\frac{m-p}{2}} T_p(z), \quad (\text{A4})$$

where e_k is 1 if k is even and 0 if k is odd.

After substituting (A4) and (A3) into (A1), changing the order of summation will analytically continue the circular region of convergence of (A1) into the wider one defined by the restriction that $z-z_p \notin (-1,1)$. Finally, after shifting the summation index we have

$$V_n(z-z_p) = \sum_{s=0}^{\infty} (-1)^n \epsilon_s \sum_{m=0}^{\infty} \frac{(2m+s+n-1)!}{m!(m+s)!(n-1)!} \\ \times V_{n+2m+s}(z_p) {}_2F_1(2m+s+n, 2m+s; n \\ +1; V_2(z_p)) T_s(z). \quad (\text{A5})$$

Comparison with Eq. (12) gives

$$\beta_s^n(z_p) = (-1)^n \epsilon_s \sum_{m=0}^{\infty} \frac{(2m+s+n-1)!}{m!(m+s)!(n-1)!} \\ \times V_{n+2m+s}(z_p) {}_2F_1(2m+s+n, 2m+s; n \\ +1; V_2(z_p)). \quad (\text{A6})$$

2. Differentiation of the monopole

The most physically meaningful method of derivation relies on the expansion of the field due to a monopole (i.e., the two-dimensional Green's function for Laplace's equation) in terms of the elliptical basis functions ("elliptical multipoles"): $\cosh^{-1}z, V_1(z), V_2(z), \dots, V_r(z)$.

From [14],

$$-\ln(z-z_p) = -\ln \frac{1}{2} - \cosh^{-1} z_p + \sum_{r=1}^{\infty} \frac{2}{r} T_r(z) V_r(z_p) \quad (\text{A7})$$

$$= -\ln \frac{1}{2} - w_p + \sum_{r=1}^{\infty} \frac{2}{r} \cosh(rw) e^{-rw_p}, \quad (\text{A8})$$

where $z = \cosh w = \cosh(\mu + i\theta)$ and $z_p = \cosh w_p = \cosh(\mu_p + i\theta_p)$. This series representation is convergent provided that $\mu_p > \mu$. It is interesting to note that $\cosh^{-1}z_p$ plays the role of the monopole in elliptical coordinates.

This equation can be differentiated with respect to the source point, z_p , to generate expansions of the higher-order multipoles. In particular, we have the dipole expansion

$$\frac{1}{z-z_p} = -\frac{1}{\sinh w_p} - \frac{1}{\sinh w_p} \sum_{r=1}^{\infty} 2 \cosh(rw) e^{-rw_p} \quad (\text{A9})$$

$$= -\sum_{r=0}^{\infty} \epsilon_r \cosh(rw) \frac{e^{-rw_p}}{\sinh w_p}. \quad (\text{A10})$$

Continuing this process we have, for $k > 0$,

$$\frac{(k-1)!}{(z-z_p)^k} = -\sum_{r=0}^{\infty} \epsilon_r \cosh(rw) \frac{\partial^{k-1}}{\partial z_p^{k-1}} \left(\frac{e^{-rw_p}}{\sinh w_p} \right). \quad (\text{A11})$$

When these expressions are substituted into the Laurent expansion (valid for $|z-z_p| > 1$),

$$V_n(z-z_p) = \sum_{k=0}^{\infty} \frac{n^{(2k)} 2^{-n-2k}}{(n+1)^{(k)} k!} (z-z_p)^{-n-2k}, \quad (\text{A12})$$

and the appropriate comparison made with Eq. (12), we obtain

$$\beta_s^n(z_p) = \frac{\epsilon_s}{s} \sum_{k=0}^{\infty} \frac{n^{(2k)} 2^{-n-2k}}{(n+1)^{(k)} k! (n+2k-1)!} \\ \times \frac{\partial^{n+2k}}{\partial z_p^{n+2k}} V_s(z_p), \quad s > 0, \quad (\text{A13})$$

and for $s=0$

$$\beta_s^n(z_p) = -\sum_{k=0}^{\infty} \frac{n^{(2k)} 2^{-n-2k}}{(n+1)^{(k)} k! (n+2k-1)!} \frac{\partial^{n+2k}}{\partial z_p^{n+2k}} \cosh^{-1} z_p. \quad (\text{A14})$$

The repeated derivative of the function $V_s(z_p)$ is a known function (preceding section) and the repeated derivative of $\cosh^{-1}z_p$ can be evaluated using the Rodriguez formula for the Gegenbauer polynomials [15]. So, after substituting and noting that the two cases $s=0$ and $s>0$ may be combined, we have

$$\beta_s^n(z_p) = (-1)^n \epsilon_s \sum_{m=0}^{\infty} \frac{n(2m+s+n-1)!}{m!(m+n)! s!} \\ \times V_{n+2m+s}(z_p) {}_2F_1(2m+s+n, 2m+n; s \\ +1; V_2(z_p)). \quad (\text{A15})$$

This is similar in form to the series obtained in the preceding section (A6), although it is not clear how their equivalence can be proved directly.

APPENDIX B: REDUCTION TO THE CIRCULAR RAYLEIGH IDENTITY

It is a relatively straightforward matter to reduce the elliptical Rayleigh identity (31),(32) to the circular Rayleigh identity [1] by allowing the coordinate eccentricity c to tend to zero and in so doing transform the elliptical coordinates into circular ones.

First, for a fixed z and $c \rightarrow 0$ the coordinate transform $z = c \cosh w$ implies that $\mu = \text{Re}(w)$ becomes very large and so $z \rightarrow ce^w/2$. This is the polar coordinate transform $z = re^{i\phi}$ with $r = ce^\mu/2$ and $\phi = \theta$.

The above results imply that for fixed z and $c \rightarrow 0$, $V_n(z/c) \rightarrow (c/2z)^n$ and $T_n(z/c) \rightarrow 1/\epsilon_n(2z/c)^n$, so that the field expansions (5),(4) reduce to

$$\mathcal{V}_e(z) = A_0 + \sum_{n=1}^{\infty} [A_n z^n + B_n z^{-n}], \quad (\text{B1})$$

$$\mathcal{V}_i(z) = \sum_{n=0}^{\infty} C_n z^n. \quad (\text{B2})$$

These are the field expansions used in [1] to solve the circular problem and so it is evident that the elliptical coefficients

$A_s^e, A_s^o, B_s^e, B_s^o, C_s^e, C_s^o$ tend to precisely the circular coefficients used by Rayleigh [1]. Therefore, the boundary conditions (27–30) simplify (for $s > 0$) to

$$A_s^{(e,o)} = \frac{e^{s\mu_0} + \epsilon e^{s\mu_0}}{(1-\epsilon)e^{2s\mu_0}} \left(\frac{2}{c}\right)^{2s} e^{-s\mu_0} B_s^{(e,o)}, \quad (\text{B3})$$

$$C_s^{(e,o)} = \frac{2}{(1-\epsilon)e^{2s\mu_0}} \left(\frac{2}{c}\right)^{2s} B_s^{(e,o)}. \quad (\text{B4})$$

After making the identification $e^{\mu_0} \rightarrow 2r_0/c$, where r_0 is the radius of the circular inclusion, these reduce further to give

$$A_s^{(e,o)} = \frac{1+\epsilon}{1-\epsilon} r_0^{-2s} B_s^{(e,o)}, \quad (\text{B5})$$

$$C_s^{(e,o)} = \frac{2}{1-\epsilon} r_0^{-2s} B_s^{(e,o)}. \quad (\text{B6})$$

These are identical to those used by Rayleigh [1] and others in solving the circular problem.

Finally, to show that the field identity (21) reduces to the correct form, consider

$$\begin{aligned} \frac{1}{\epsilon_s} \left(\frac{2}{c}\right)^{n+s} \beta_s^n \left(\frac{z_p}{c}\right) &= (-1)^n \left(\frac{2}{c}\right)^{n+s} V_{n+s} \left(\frac{z_p}{c}\right) \sum_{m=0}^{\infty} \frac{(2m+s+n-1)!}{m!(m+s)!(n-1)!} V_{2m} \left(\frac{z_p}{c}\right) {}_2F_1 \left(2m+s+n, 2m+s; n+1; V_2 \left(\frac{z_p}{c}\right)\right) \\ &\rightarrow (-1)^n z_p^{-(n+s)} \sum_{m=0}^{\infty} \frac{(2m+s+n-1)!}{m!(m+s)!(n-1)!} \delta_{m,0} \rightarrow (-1)^n \binom{s+n-1}{s} z_p^{-(n+s)}. \end{aligned} \quad (\text{B7})$$

Therefore, after summing over the lattice we have that as $c \rightarrow 0$,

$$\sigma(n,s) \rightarrow (-1)^n \binom{s+n-1}{s} S_{n+s}, \quad (\text{B8})$$

where S_k are the circular lattice sums: $S_k = \sum_{p \neq 0} z_p^{-k}$. Using this with the field identity (21) gives

$$A_s = -\bar{E}_0 \delta_{s,1} + \sum_{n=1}^{\infty} (-1)^n \binom{s+n-1}{s} S_{n+s} B_n. \quad (\text{B9})$$

Combining these results, we have shown that the field expansions, boundary conditions, and field identity for the elliptical problem reduce precisely to those of the circular problem in the appropriate limit—a fact which has also been confirmed numerically.

APPENDIX C: MISCELLANEOUS RESULTS, GRAPHS, AND THE EXTERIOR ADDITION FORMULA

1. Miscellaneous results involving the β_s^n

In the course of studying the $\beta_s^n(z_p)$ and, in particular, the integral representation (14), it was established that $\beta_s^n(z_p)$ is

in fact some combination of elliptic functions of the third kind [8], although the precise form is unknown. Interestingly, however, in the case where $z_p = 2$, the $\beta_s^n(z_p)$ reduce to sums of elementary functions, although once again the exact formula for general n and s is unknown. Also, the special (and physically dubious) case of $z_p \rightarrow 0 + i0$ is known exactly:

$$\beta_s^n(0 + i0) = - \frac{2\epsilon_s (-1)^n i^{-n-s} n \sin \pi \left(1 + \frac{n-s}{2}\right)}{\pi(n-s)(n+s)}. \quad (\text{C1})$$

Other results include

$$\beta_s^0(z_p) = \delta_{0,s}. \quad (\text{C2})$$

Comparison between (A6) and (A15) yields a deep relationship satisfied by the β_s^n :

$$\beta_s^n(z_p) = (-1)^{n-s} \frac{n}{s} \beta_n^s(z_p), \quad s > 0. \quad (\text{C3})$$

TABLE II. Values of $\beta_s^n(2.2)$.

n/s	0	1	2	3	4	5	6
0	1.0	0	0	0	0	0	0
1	-0.28747	-0.16673	-0.052895	-0.018238	-0.0067557	-0.0026535	-0.0010917
2	0.09813	0.10579	0.047766	0.020595	0.0088342	0.0038278	0.0016842
3	-0.038516	-0.054713	-0.030893	-0.015781	-0.0076917	-0.0036704	-0.0017378
4	0.016626	0.027023	0.017668	0.010256	0.005558	0.0028925	0.0014696
5	-0.0076167	-0.013267	-0.0095695	-0.0061173	-0.0036156	-0.0020289	-0.0010996
6	0.0036202	0.0065502	0.0050527	0.0034757	0.0022045	0.0013196	0.00075768

An equivalent formula holds for the elliptical lattice sums $\sigma(n, s)$.

Also, a functional equation connecting the β_s^n was able to be derived by considering various forms of Eq. (12):

$$\beta_k^{n+m}(z_p) = \frac{1}{2} \sum_{i=0}^k \beta_i^n(z_p) \beta_{k-i}^m(z_p) + \frac{\epsilon_k}{4} \sum_{s=0}^{\infty} \beta_{s+k}^n(z_p) \beta_s^m(z_p) + \beta_s^n(z_p) \beta_{s+k}^m(z_p), \tag{C4}$$

where n and m can be any integer.

It was found that if the path of integration used in the integral representation (14) was changed from C_1 to C_3

(Fig. 8), then the integral, while nontrivial, can be evaluated in terms of elementary functions:

$$\frac{\epsilon_s}{2\pi i} \oint \frac{V_n\left(\frac{z-z_p}{c}\right) T_s\left(\frac{z}{c}\right)}{\sqrt{z+c}\sqrt{z-c}} dz = \sum_{k=0}^{\lfloor \frac{s-n}{2} \rfloor} \frac{n^{(2k)}}{(n+1)^{(k)}k!} C_{s-n-2k}^{n+2k}(z_p), \tag{C5}$$

where C_n^m is the n th Gegenbauer polynomial of the m th kind. This integral can be used to derive an elegant form for the exterior addition formula (C10).

We list here some of the results that were derived in the course of striving for a more illuminating series representation of the $\beta_s^n(z_p)$:

$$\beta_s^n(z_p) = \frac{\epsilon_s}{2} \sum_{k=0}^{\lfloor \frac{s-n}{2} \rfloor} \frac{n^{(2k)}}{(n+1)^{(k)}k!} C_{s-n-2k}^{n+2k}(z_p) - \epsilon_s \sum_{k=0}^{\infty} \frac{n^{(2k)}(\frac{1}{2})_{(n+2k)}}{(n+1)^{(k)}k!(n+2k-1)!} (z_p^2 - 1)^{1/2-n-2k} {}_2F_1 \left(s-n-2k+1, -s-n-2k+1; \frac{3}{2}-n-2k; \frac{1-z_p}{2} \right). \tag{C6}$$

TABLE III. Values of $\beta_s^n(I/5)$.

n/s	0	1	2	3	4	5	6
0	1.0	0	0	0	0	0	0
1	0.54994I	0.65647	-0.2971I	-0.067735	-0.0065786I	-0.013387	0.0039841I
2	-0.12355	0.5582I	0.47709	-0.25858I	-0.083753	0.0027602I	-0.013219
3	0.057677I	-0.2032	0.38787I	0.35764	-0.21574I	-0.082481	0.010243I
4	-0.056579	0.026314I	-0.16751	0.28766I	0.27262	-0.17527I	-0.074921
5	-0.0087316I	-0.066934	-0.0069005I	-0.13747	0.21909I	0.21007	-0.14106I
6	-0.013847	-0.023904I	-0.039656	-0.020485I	-0.11238	0.16927I	0.16313

Also, note that the first sum becomes empty when $n > s$.

Using the linear transformation rules for hypergeometric functions [8], we can express Eq. (16) in terms of terminating hypergeometric functions:

$$\begin{aligned} \beta_s^n(z_p) &= (-1)^n \epsilon_s \sum_{m=0}^{\infty} \frac{(2m+s+n-1)!}{m!(m+s)!(n-1)!} \\ &\times \frac{V_{n+2m+s}(z_p)}{(1-V_2(z_p))^{4m+2s-1}} {}_2F_1(1-2m-s, 1+n-2m \\ &-s; n+1; V_2(z_p)). \end{aligned} \quad (C7)$$

The hypergeometric functions for which quadratic transformations exist are related to Legendre functions and in particular, using the equation connecting toroidal functions with the ${}_2F_1$ (given on page 1022 of [15]) we have

$$\begin{aligned} \beta_s^n(z_p) &= (-1)^{n+s+1/2} n \epsilon_s \sqrt{\frac{2}{\pi}} \\ &\times \sum_{m=0}^{\infty} \frac{2^{-2m-s}}{m!(m+s)!} \frac{Q_{n-1/2}^{2m+s-1/2}(z_p)}{(\sqrt{z_p^2-1})^{2m+s-1/2}}. \end{aligned} \quad (C8)$$

If the Gegenbauer functions of the second kind are used [14], then we have

$$\begin{aligned} \beta_s^n(z_p) &= (-1)^{n+s+1/2} n \epsilon_s \\ &\times \sqrt{\frac{2}{\pi}} \sum_{m=0}^{\infty} \frac{2^{-2m-s}}{m!(m+s)!} V_{n-2m-s}^{2m+s-1/2}(z_p). \end{aligned} \quad (C9)$$

2. Tables and graphs of the $\beta_s^n(z_p)$

Tables II and III contain the values of $\beta_s^n(z_p)$ for certain representative values of z_p calculated to a precision of five significant figures. In both these examples, the integral representation (15) was used to calculate the $\beta_s^n(z_p/c)$ with $c = 1$.

Table II is for the case $z_p = 2.2$, which corresponds to the situation where the branch cuts (and therefore ellipses) are almost touching along the x direction. Alternatively, Table

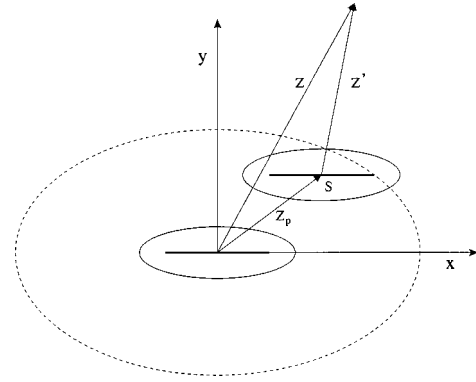


FIG. 14. Geometry of the exterior addition formula.

III shows the case where the branch cuts are almost touching along the y axis.

Table III show the trend in which along the bottom row or down the rightmost column the magnitude of β_s^n is increasing. While this is true, it is still the case that for any fixed row or column, as the other index gets large the magnitude of β_s^n tends to 0. Indeed, the magnitudes are bounded by those down the main diagonal and these are uniformly decreasing.

3. The exterior addition formula

The exterior addition formula enables a field, the sources of which are located on the branch cut centered on S (see Fig. 14), to be expanded in terms of the functions $V_s(z/c)$. The restriction on its applicability is that the field point must lie outside the smallest ellipse that completely contains the branch cut (see Fig. 14). The actual ellipses shown in Fig. 14 (solid lines) are nothing more than a decoration—it is the position of the branch cut at S and the field point that determine the convergence properties of the exterior addition formula. Indeed, the solid ellipses may intersect or even overlap without necessarily effecting the convergence of the addition formula:

$$V_n\left(\frac{z-z_p}{c}\right) = \sum_{s=0}^{\infty} \left[\sum_{k=0}^{\lfloor \frac{s-n}{2} \rfloor} \frac{n^{(2k)}}{(n+1)^{(k)}k!} C_{s-n-2k}^{n+2k}\left(\frac{z_p}{c}\right) \right] V_s\left(\frac{z}{c}\right). \quad (C10)$$

[1] Lord Rayleigh, *Philos. Mag.* **34**, 481 (1892).
 [2] G. K. Batchelor, *Annu. Rev. Fluid Mech.* **6**, 227 (1974).
 [3] N. A. Nicorovici and R. C. McPhedran, *Phys. Rev. E* **54**, 1945 (1996).
 [4] A. R. Forsyth, *Theory of Functions of a Complex Variable* (Cambridge University Press, Cambridge, UK, 1893).
 [5] Shih-Yuan Lu, *J. Appl. Phys.* **76**, 2641 (1994).
 [6] J. Keller, *J. Appl. Phys.* **34**, 991 (1963).
 [7] J. Keller, *J. Math. Phys.* **5**, 548 (1964).
 [8] *Handbook of Mathematical Functions with Formulas, Graphs and Mathematical Tables*, edited by M. Abramowitz and I. A. Stegun (Dover, New York, 1972).
 [9] C. G. Poulton, L. C. Botten, R. C. McPhedran, and A. B.

Movchan (unpublished).
 [10] J. A. Beunen, M.Sc. thesis, University of Sydney, 1976.
 [11] W. T. Perrins, D. R. McKenzie, and R. C. McPhedran, *Proc. R. Soc. London Ser. A* **50**, 207 (1979).
 [12] Abdel-Razik Sebak, *IEEE Trans. Antennas Propag.* **42**, 1521 (1994).
 [13] Staff of the Bateman Manuscript Project, *Higher Transcendental Functions* (McGraw-Hill, New York, 1953), Vol. 2.
 [14] P. M. Morse and H. Feshbach, *Methods of Theoretical Physics* (McGraw-Hill, New York, 1953).
 [15] I. S. Gradshteyn and I. M. Ryzhik, *Table of Integrals, Series, and Products*, 4th ed. (Academic Press, New York, 1965).